Advances in Energy Science and Technology
Vol. 1, No. 2|1 September 2025
AEST

Performance Evaluation of PCM InfiniteR29 and Its Impact on a Single-Family Residential Building: A Case Study in Jinan, China

MohammadReza Mehdizadeh Marzebali[a], **Masoumeh Mohamadian**[a,*]

[a] Amirkabir University of Technology, Tehran, Iran

Keywords

Passive Strategy
Phase Change Materials
DesignBuilder
Energy Consumption
Indoor Temperature
PCM Integration

* **Masoumeh Mohamadian:** mohamadian@aut.ac.ir

Abstract

Global warming and climate change, primarily driven by CO_2 emissions from building energy consumption, pose significant environmental challenges. This study investigates the energy performance of a single-family residential building in Jinan, China—a city characterized by a temperate monsoon climate—using simulation-based methods. The baseline building model was developed in DesignBuilder, leveraging the EnergyPlus engine to estimate annual electricity, heating, and cooling demands. To enhance passive energy efficiency, Phase Change Material (PCM), specifically InfiniteR29, was incorporated into the external walls and roof. The impact of PCM integration was evaluated in terms of envelope heat flux, overall energy loads, and indoor air temperature regulation. Results indicate that the inclusion of PCM reduces annual heat flux through the building envelope by 19.7%, leading to reductions of 12.7% in heating load and 45.6% in cooling load. Furthermore, PCM application significantly moderates indoor temperature fluctuations during extreme weather conditions, achieving a peak temperature reduction of 2.4°C during summer and exhibiting a thermal lag effect. These findings confirm that properly selected PCMs can substantially improve envelope thermal stability, lower energy consumption, and enhance passive building performance in climates with substantial seasonal and diurnal temperature variations.

Graphical Abstract

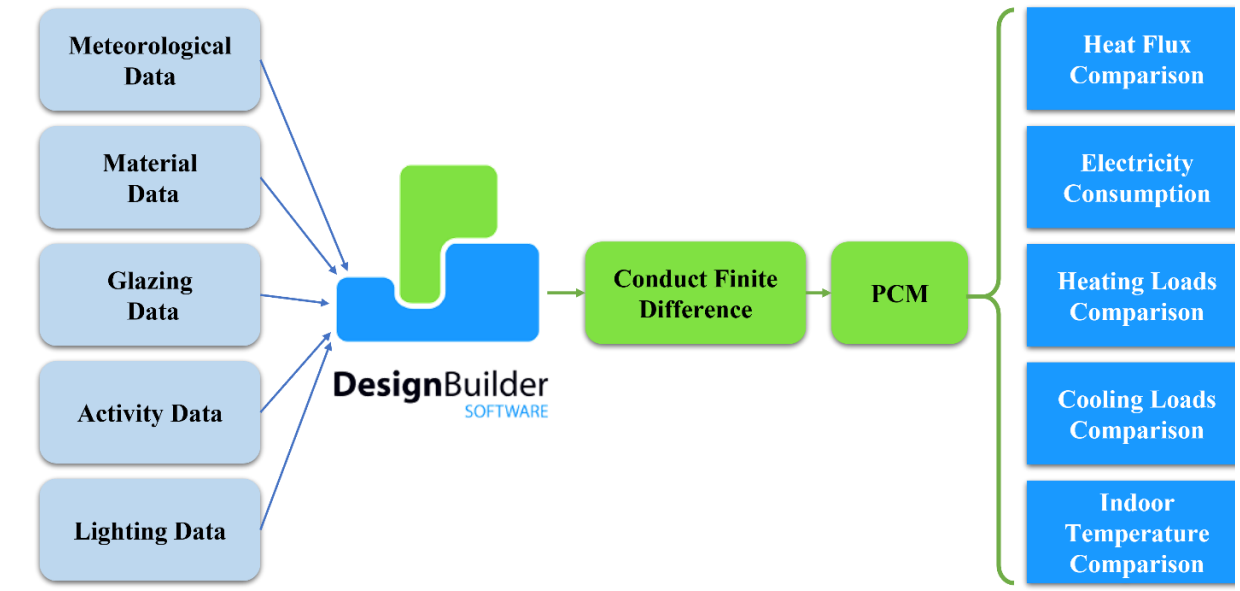

1. Introduction

1.1. Motive and Solution

Over recent decades, CO_2 emissions have become a critical global concern, motivating the European Union (EU) to implement assertive objectives and policies to combat climate change [1] and [2]. Directive 2018/2002/EU's "Clean energy for all Europeans" initiative sets a goal to significantly enhance energy efficiency and reduce reliance on non-renewable energy sources by 32.5% by the year 2030 [3]. Demonstrating a commitment to a 55% emission reduction by 2030 and climate neutrality by 2050, the EU is intently addressing energy consumption, especially within the building sector [1]. With ongoing population growth, urbanization, and economic development, energy demand from buildings is expected to keep rising [4]. For example, in 2021, building energy consumption increased by 3% and CO_2 emissions by 5% compared to the previous year [4]. Worldwide concern over climate change drives extensive research into reducing building energy consumption, as structures account for 34% of global final energy consumption and 37% of CO_2 emissions [5]. Considering the building sector's substantial carbon emissions, decarbonization strategies are intensifying to boost energy efficiency and reduce overall energy consumption and greenhouse gas output [2].

To address these issues, international strategies include minimizing solar heat gain with reflective coatings, new insulation materials, air gaps in walls, and integrating PCMs into buildings [5]. PCM-based solutions can be incorporated into buildings in various manners, including passively as integrated layers within the building envelope or actively as components of HVAC systems [1]. PCMs, available as either organic or inorganic substances, possess the capacity to store and release significant thermal energy during a phase change (such as transitioning from solid to liquid) with only minor temperature changes [6].

1.2. Literature Review

PCMs have extensive applications in reducing energy consumption and achieving zero carbonization, whether in buildings or out-of-building sectors. Shah et al. studied a concentrated photovoltaic system with paraffin-based PCM (58°C melting point) to improve thermal storage and efficiency in hot climates. The PCM lowered panel temperature by 40°C, boosting energy output by 30% and annual electrical yield by 5.9%. A numerical model optimized the PCM melting point and container size under UAE's high solar radiation [7]. Sacchet et al. improved PCM stabilization using expanded graphite in photovoltaic cells. Three PCMs (RT35, RT44, fatty acid eutectic) were vacuum-impregnated into 6×6×2 cm panels. Thermal conductivity reached 6 W/m·K, melting enthalpy 160–220 J/g, and leakage was reduced 10×, confirming effectiveness for passive cooling [8]. Jia et al. investigated PCM-functionalized demolition waste aggregate to improve concrete durability. The modified concrete increased durability by 31.5%, showed zero carbonation depth, enhanced freeze-thaw resistance, and reduced chloride penetration by 9.4% and sulfate-induced mass loss by 11.8% [9].

PCMs have been extensively studied for their use in HVAC systems to decrease energy consumption in structures and improve thermal comfort by moderating temperature swings [6]. PCMs are notable for their ability to lower HVAC peak loads and improve operational efficiency [4]. Gad et al. studied a hybrid cooling system with heat pipes and PCM in Egypt. SP31 (3 cm) cut PV temperature by 20.6°C, boosting efficiency 11.5%; SP15-gel (2.5 cm) reduced temperature by 14.1°C with a 7.2% gain. Exergy analysis showed 13.4% max daily efficiency; payback dropped from 18.01 to 13.39 years, confirming system viability [10]. Lazzarin et al. studied PCM thermal storage with aluminum foam for solar heating and heat pumps. PCM with foam improved heat transfer by 83%, reducing charge times. PCM systems cut energy costs by 27% and payback from 18.01 to 13.39 years, confirming viability for near-zero-energy buildings [11]. Kandil et al. explored

passive cooling for buildings using PCM-based phase cubes. Testing six PCM compact storage module (PCM-CSM) designs at 35°C and 4 m/s, the horizontal PCM-CSM absorbed 496.19W, dropping the outlet air to 25°C. Integrating PCM-CSMs cuts cooling loads, reducing air conditioning energy use up to 40%, supporting net-zero energy buildings [12].

Notably, the translucent envelope, a key component in building heat balance, accounts for roughly 25% to 40% of heating and cooling energy needs [2]. In recent years, the scientific community has shown considerable interest in research concerning the integration of PCMs into building envelopes, owing to their remarkable capabilities in diverse heat transfer and energy storage applications [13]. Mandev studied double-glazed windows with PCM and black film coatings for thermal regulation. A 45% PCM area cut peak indoor temperature by 3.9°C during heating. Black films raised the temperature by 2.6°C but reduced light transmittance by 68%. The study highlights balancing thermal comfort and natural lighting for energy-efficient glazing [14]. The incorporation of PCM into a building's wall modifies the temperature profile through the wall, consequently influencing heat transfer to the interior space [15]. The effectiveness of these building walls depends crucially on the PCM's exact position within the wall, its melting temperature, and the specific thickness of the PCM layer [15]. Considering these variables, numerical simulations have been executed for a typical building wall, with the resulting data reported in terms of the PCM's melt fraction and the heat flux at the internal wall surface [15]. Özdemir and Gülten studied PCM effects on heating/cooling loads in brick, concrete block, and aerated concrete walls across 39 scenarios with PCM melting points of 21°C, 23°C, and 29°C. PCM plus XPS insulation cut annual energy demand by 30% and PCM alone saved 9%. They recommend dual melting point PCM for optimal thermal regulation [16]. Krasoń et al. studied four Trombe wall designs, three with PCM to improve thermal storage. Experiments showed PCM walls extended heat release by up to 10 hours and reduced indoor temperature swings by 6.2°C. Statistical analysis confirmed PCM walls stored 14% more heat and lowered peak heat flux by 28%, enhancing energy efficiency and comfort [17]. Ryms and Klugmann-Radziemska tested three PCM methods for hollow-brick walls, including microcapsule powder, liquid PCM, and porous aggregate. The aggregate method extended cooling time by 95 percent and achieved nearly 100 percent temperature stabilization while reducing fluctuations cost-effectively compared to microencapsulated PCM [18].

1.3. Objective of the study

Numerous studies have explored PCM applications in building materials, facades, and envelope systems. However, most have focused on isolated components, small-scale test cells, or very specific climatic conditions. Additionally, many investigations have emphasized theoretical analyses without validating the real-world implications through full-building simulations over an extended period. To address these limitations, the current study conducts a high-resolution, annual simulation of a real-sized residential building located in a temperate monsoon climate. Using the DesignBuilder interface and EnergyPlus engine, this research evaluates the impact of integrating InfiniteR29 PCM with experimental specification into both the walls and the roof of the building. Unlike prior work that primarily focuses on either wall assemblies or abstract models, this study provides a comprehensive assessment of PCM effectiveness at the whole-building level. The novelty of this research lies in its integrated approach to simulate and compare the thermal behavior of the envelope, specifically heat flux and indoor temperature patterns, between base and PCM-enhanced cases throughout the entire year. This holistic view contributes valuable data-driven insights to the body of knowledge on passive energy-saving measures for climate-responsive architecture.

2. Methodology

The study models a real-scale residential building in Jinan using DesignBuilder with EnergyPlus. Heating, cooling, and electric loads were computed under base and PCM-enhanced scenarios. InfiniteR29 PCM with experimental specification was applied to the walls and roof (5 cm thickness). Then the walls and roof are investigated in heat flux, consumption, and indoor temperature of the building. No HVAC systems were simulated; thus, results refer to thermal loads rather than delivered energy. Graphical abstract presents the workflow of the adopted methodology.

2.1. Climate and Weather

For this study, Jinan city in China is selected as the climate of the residential building, which is shown in **Fig. 1** Jinan, located at 36°40′ N and 117°00′ E in eastern Shandong Province [19], sits in a colder region of China and features a temperate monsoon climate characterized by cold winters and hot, humid summers [20]. The city's strategic position on the Shandong Peninsula, adjacent to the North China Plain, influences both its climate and agricultural landscape. Its geography is further defined by Mount Tai to the south, a site of cultural and historical significance, and the Yellow River to the north. Administratively, Jinan is divided into 12 districts and counties [21].

Fig. 1. Jinan's geographical climate.

Throughout the year, prevailing winds mostly come from the southwest and east [19], and the city's annual mean temperature is 14.9 °C [19], with recorded extremes ranging from –11 °C to 37.2 °C [19]. The year is divided into three main thermal seasons: the heating season spans January to March and November to December, when temperatures are low and heating is required; the cooling season is limited to July and August, the hottest months; and the shoulder season, with milder weather, covers April to June and September to October [22]. Between late May and early September, Jinan experiences hot and humid conditions, with typical outdoor temperatures between 26 °C and 31 °C [22]. Summers (June–August) often see temperatures above 30 °C (sometimes exceeding 35 °C), humidity above 70% [20], and solar radiation between 600–

800 Wh/m² [20], while winters (December–February) are cold and dry, with average temperatures of 2–3 °C, lows near –12 °C, humidity below 50% [20], and solar radiation mostly 200–400 Wh/m² [20]. Direct solar irradiance in winter is reduced by 30–40% compared to summer levels [22], and the solar incidence angle during winter ranges from 5° to 78° [23]. Due to these climatic conditions, Jinan has considerable annual energy consumption for both heating and cooling, which the study aims to reduce. The weather data for Jinan was obtained in EPW format from the EnergyPlus Weather Data website and imported into DesignBuilder for simulation. **Fig. 2** presents the hourly outdoor temperature and the monthly averages of solar radiation and clearness index for Jinan, based on the referenced climate data.

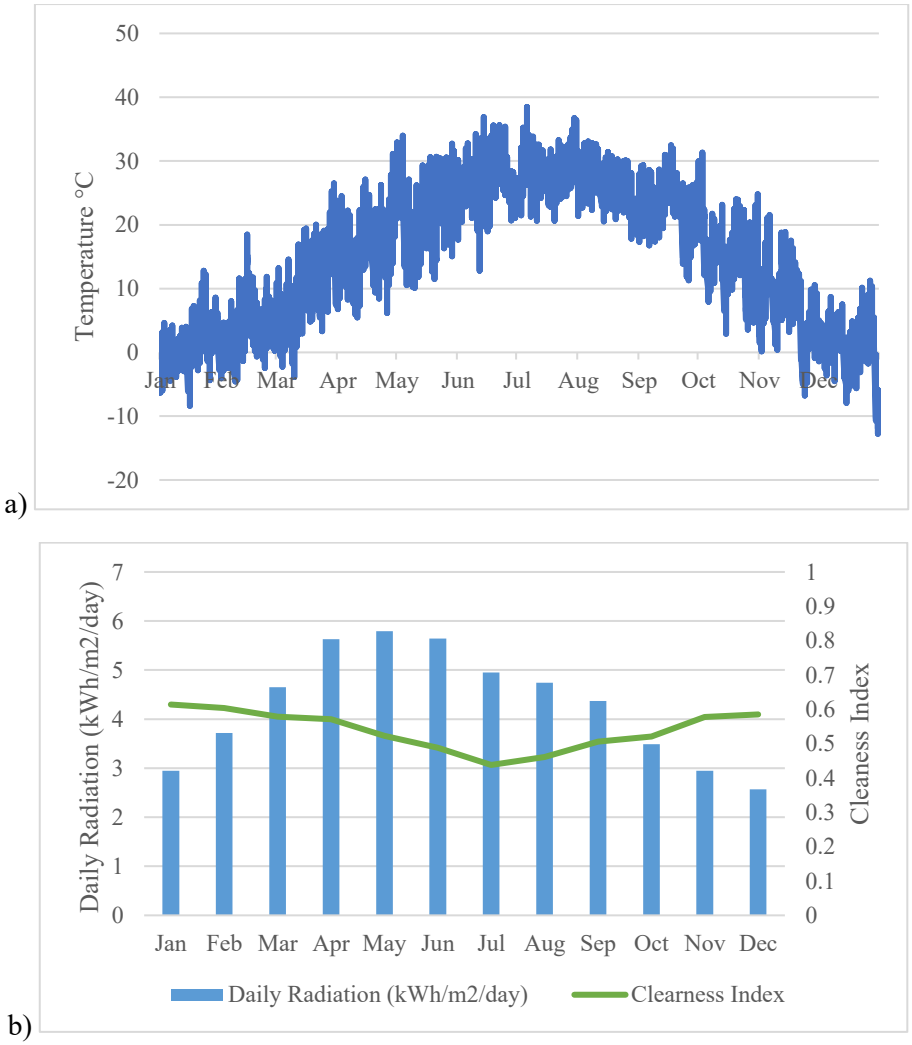

Fig. 2. Weather of Jinan: a) Dry bulb temperature. b) Solar radiation in Jinan.

2.2. Case study

This study focuses on a north-oriented single-family house, designed to evaluate its energy performance through simulation. The building has a floor area of 86 m² with a ceiling height of 3.3 m and features five double-glazed windows, each measuring 1.5 m × 1.5 m and positioned 1.2 m above floor level. The house comprises two bedrooms, a kitchen combined with a dining room, a living room, a WC, and a bathroom, providing a typical residential layout. The simulation considers climate data, lighting specifications, building materials, and activity-related parameters, such as heating and cooling setpoints for indoor

comfort temperature, as well as internal gains for each thermal zone. **Fig. 3** shows the plan of that residential building with defined thermal zones on the plan.

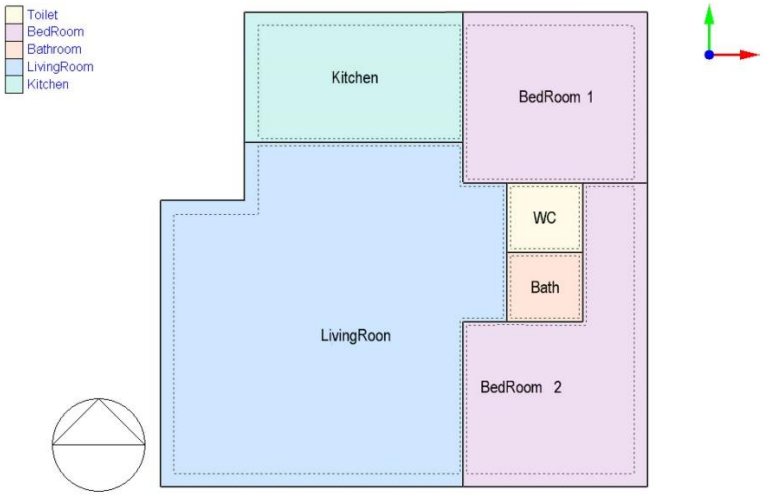

Fig. 3. Plan and thermal zone of the single home.

Thermal zones are categorized according to functional spaces, with metabolic rates of occupants assigned accordingly. The building accommodates four occupants [24], [25], [26], with an average occupancy density of 0.05 p/m² [27]. In this simulation, two individuals occupy the bedrooms, one person stays in the kitchen, and one in the living room. The electrical consumption is recorded as follows: 3.9 W/m² in the living room [28], 3.6 W/m² for bedroom equipment [28], 1.7 W/m² in the bathroom [28], and 10 W/m² in the kitchen, mainly due to catering operations [24]. The occupants follow a predefined electricity usage schedule, operating these appliances between 00:00 – 08:00 and 18:00 – 24:00, which is suitable for residential application [29].

For lighting efficiency, the house is equipped with energy-efficient LED lamps [27], [24], [25], maintaining an illumination level of 150 lux [26]. Domestic hot water (DHW) consumption is calculated at 0.72 l/m² [24], with a water delivery temperature of 50°C [24]. The infiltration rate is set to 0.7 air changes per hour [26], [27], ensuring appropriate ventilation levels. The window consists of two distinct glazing layers. The exterior layer features 0.3 cm PYR B Clear Glass with a thermal conductivity of 0.9 W/m·K, while the interior layer includes 0.3 cm clear glass with the same conductivity [30]. A 1.3 cm air gap separates them, enhancing insulation and energy efficiency. Table 1 shows the data modeling of the building.

Table 1. Specifications of the simulated building.

Category	Parameters	Value	Reference
Building envelope	North wall area	34.90 m^2	-
	South wall area	34.90 m^2	
	East wall area	34.05 m^2	
	West wall area	34.08 m^2	
	Roof area	101.7 m^2	
HVAC system	The heating set point temperature	24	[24]
	The heating setback temperature	22	
	The cooling set point temperature	28	[26]
	The cooling setback temperature	30	
	Mechanical ventilation rate for fresh air	0.06 CFM/sq^2 ≈ 0.3 l/s.m^2	[31]
Lighting system	Lighting power	7.5 W/m^2	[26], [27]
	Lighting work plane height	0.8	[26]
Glazing (Double glazed)	Glazing to wall ratio	8.16 %	-
	U-Value of the pane	1.96 W/m^2.K	

	Solar transmittance PYR B Clear Glass	0.74	[30]
	Visible transmittance PYR B Clear Glass	0.82	
	Solar transmittance Clear Glass	0.837	
	Visible transmittance Clear Glass	0.898	

The building materials were documented based on the initial architectural phase, serving as the primary reference for construction specifications and material analysis (Source: Internal architectural records). Their thermal and structural properties are detailed in the specifications Table 2, with the shading reflectance of 0.4 [26].

Table 2. Building envelope specifications.

Façade Envelope	Composition	Thickness [cm]	Thermal conductivity [W/m.K]	Specific heat capacity [J/kg.K]	Density [kg.m^3]	Reference
Wall (exterior to interior)	Stone	2	2.8	1000	2600	[32]
	Cement Mortar	2	1.15	1000	1700	[30]
	Hollow-Brick	20	0.72	840	1920	[33]
	Plaster	1.5	1	900	1800	[34]
	Gypsum Plaster	1	0.51	960	1120	[32]
Roof (exterior to interior)	Bitumen	3	٠,٥	١٠٠٠	١٧٠٠	[30]
	Cement Mortar	2	1.15	1000	1700	[30]
	Lightweight concrete	5	٠,٦	٨٤٠	١٤٠٠	[34]
	Reinforcement Concrete	15	٢,٣	١٠٠٠	٢٣٠٠	[34]
	Plaster	1.5	1	900	1800	[34]
	Gypsum Plaster	1	0.51	960	1120	[32]

2.3. Design Builder Software

DesignBuilder, a graphical interface powered by the EnergyPlus simulation engine, is widely used for analyzing dynamic building energy performance. EnergyPlus is recognized for its accuracy in modeling energy behavior, making it a trusted tool in sustainable building design and energy efficiency research. DesignBuilder supports detailed input of thermal properties, building features, and material data to reliably estimate annual heating and cooling energy demands [35]. After establishing the numerical model in DesignBuilder, the software calculates the yearly energy requirements for heating and cooling systems. This process aids engineers and researchers in evaluating energy consumption patterns and optimizing HVAC system designs for specific applications [36, 37]. Furthermore, simulation platforms such as EnergyPlus, TRNSYS, and DesignBuilder have been instrumental in modeling energy conservation measures under various scenarios, enabling refinement and customization of system configurations [38]. DesignBuilder enables simulation of energy use before and after applying various architectural and material strategies to enhance building thermal performance. These include diverse passive and active measures that regulate indoor conditions and reduce heating and cooling demands. This helps researchers evaluate energy optimization techniques and supports designing more efficient, sustainable buildings [39].

To conduct the energy simulation, Design Builder software is implemented to model the geometry and simulate energy performance using the EnergyPlus engine. To facilitate a detailed analysis, the building was exported to Design-Builder using the gbXML extension file [39]. **Fig. 4**. shows the schematic (3D modeling) of the simulated building in the Design Builder software.

Advances in Energy Science and Technology
Vol. 1, No. 2|1 September 2025
AEST

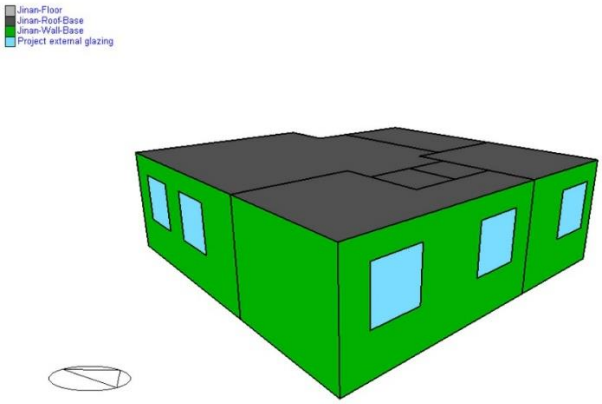

Fig. 4. A single-family house schematic is designed.

2.4. PCM characterization

PCMs provide an efficient mechanism for storing and releasing thermal energy, relying on their ability to shift between solid and liquid phases. This property enables consistent temperature regulation, making them highly effective in thermal energy storage systems (TES) across building insulation, cooling technologies, and solar energy optimization [40]. Categorized into organic, inorganic, and eutectic types, these materials exhibit distinct thermal characteristics tailored for diverse applications. Organic PCMs, including paraffins and fatty acids, offer stable thermal transitions but lower conductivity, while inorganic variations, such as salt hydrates and metallics, deliver higher thermal performance but require encapsulation for stability [41]. Eutectic PCMs, blending organic and inorganic components, present precise heat absorption and release properties suitable for specialized energy demands [41]. Innovations in PCM efficiency focus on enhancing heat transfer properties, improving phase stability, and integrating these materials into architectural structures [42]. Advancements such as nanoparticle-infused composites, encapsulation techniques, and hybrid formulations significantly refine PCM effectiveness, ensuring reliable long-term temperature regulation in diverse industries [42]. Sustainable PCM development prioritizes biodegradable and recyclable formulations, supporting eco-friendly thermal energy storage solutions. These ongoing advancements reinforce PCMs as essential components in modern temperature control technologies, contributing to optimized energy efficiency and environmental sustainability [43].

Design Builder software leverages the EnergyPlus engine for simulations, employing the conduction finite difference (ConFD) algorithm to solve heat transfer equations. This approach uses a fully implicit method that discretizes the building into multiple nodes. At each node, the one-dimensional heat transfer equations are solved individually. The **Eq. (1)** to **Eq. (4)** express the relationships governing these heat transfer processes at each node [44]:

$$\rho \cdot C_p \frac{\partial T}{\partial t} = K \frac{\partial^2 T}{\partial x^2} \tag{1}$$

$$(\rho \cdot C_p)_n \cdot \Delta x \cdot \frac{T_n^{t+1} - T_n^{t}}{\Delta t} = (K_{n+1} \cdot \frac{T_{n+1}^{t+1} - T_n^{t+1}}{\Delta x} + K_{n-1} \cdot \frac{T_{n-1}^{t+1} - T_n^{t+1}}{\Delta x}) \tag{2}$$

$$K_{n+1} = \frac{K_{n+1}^{t+1} + K_{n}^{t+1}}{2} \quad (3)$$

$$K_{n-1} = \frac{K_{n-1}^{t+1} + K_{n}^{t+1}}{2} \quad (4)$$

Where, C_p stands for specific heat, ρ stands for density, K is the symbol of thermal conductivity, while the scripts 't' and 'n' denotes the time 't' , and the 'n^{th}' node, respectively. Δx indicates the grid size of the simulation and Δt represents the timestep, while the time step is supposed to be 1 min, and Δx is computed by the **Eq. (5)** below [44]:

$$\Delta x = \sqrt{C \cdot \alpha \cdot \Delta t} \quad (5)$$

Where C usually ranging between 1 and 3 represents a constant and α is the thermal diffusivity. In this study, infiniteR29 [45] is selected as PCM with a thickness of 5cm [41] to incorporate in external walls and roof. The experimental specification of the infiniteR29 is shown in Table 3. [45]:

Table 3. Characterization of PCM InfiniteR29.

Melting point (°C)	29
Specific Heat (kJ/kg)	3.14
Latent Heat (J/g)	200
Thermal conductivity (W/m.k)	0.54 (Liquid)
	1.09 (Solid)
Density (kg/m^3)	@ 20 °C 1434.70 kg/m^3
	@ 30 °C 1433.58 kg/m^3
	@ 45 °C 1430.23 kg/m^3

2.5. Limitations and Future Research

This study provides a detailed simulation-based analysis of PCM performance; however, certain limitations should be acknowledged to contextualize the findings and guide future work. Limitations of the current study are as follows:

- Reliance on Simulation: The results presented are entirely derived from numerical simulations using the EnergyPlus engine. While this is a powerful and validated tool, the study lacks experimental validation to corroborate the predicted energy savings and thermal behavior in a real-world physical setting.
- Deterministic Occupant Behavior: The model assumes standardized, scheduled profiles for occupancy and internal gains (e.g., lighting and equipment). This approach does not account for the stochastic and dynamic nature of actual occupant behavior, which can significantly impact building energy performance.
- Single PCM Type: The investigation is confined to a single type of phase change material, InfiniteR29, with a specific melting point (29°C) and thickness (5 cm). The potential performance of other PCMs with different thermophysical properties was not explored.

3. Results

This section first quantifies and compares the heat flux through the building envelope, specifically the walls and roofs, between the base and PCM cases. Subsequently, the building's electricity consumption for lighting and equipment is evaluated alongside heating and cooling loads. The effects of PCM on thermal loads are analyzed, acknowledging that

changes in heating and cooling demands depend on various factors and may not directly mirror heat flux reductions. Monthly and seasonal variations are also discussed to comprehensively assess PCM's impact on building thermal performance. To quantify PCM effectiveness, indoor air temperature serves as the final performance metric.

3.1. Heat Flux

This section examines heat flux through the building's external walls and roof, comparing the base case without PCM and the PCM-enhanced case to evaluate its impact on heat transfer. **Fig. 5** illustrates the monthly heat flux for both the external walls and the roof in the base and PCM cases.

The values represent the sum of the absolute hourly heat fluxes aggregated monthly, with negative signs assigned to heating-dominated (winter) months (October–April) and positive signs to cooling-dominated (May–September) months to reflect the prevailing thermal load direction. Negative heat flux indicates heat loss in winter, while positive values signify heat gain in summer, increasing cooling demand and potential overheating. Optimal thermal performance is achieved when flux values are closer to zero, as this reflects minimized heat transfer. PCM integration helps regulate flux, reducing heat loss in winter and heat gain in summer, thereby enhancing energy efficiency and indoor comfort. Summing absolute hourly heat flux values accurately represents a building's thermal load, preventing underestimation due to offsetting heat gains and losses. This method is crucial for assessing PCM integration effects.

The highest heat fluxes were observed in January and July, corresponding to peak heating and cooling periods, respectively. Specifically, in January, the wall heat flux decreased from -1.59 MWh in the Base case to -1.41 MWh with PCM integration, reflecting an 11.4% reduction in heating load. Similarly, the roof heat flux declined from -1.8 MWh to -1.62 MWh, indicating a 10.2% reduction. During the peak summer month of July, PCM reduced the wall cooling load by 11.3%, from +1.21 MWh to +1.07 MWh, and the roof cooling load by 12.1%, from +1.4 MWh to +1.23 MWh. The lowest heat fluxes were recorded in April for walls (-1.11 MWh Base, -0.97 MWh PCM) and in September for roofs (+1.24 MWh Base, +1.07 MWh PCM), with PCM yielding reductions of approximately 12.5% and 13.6%, respectively.

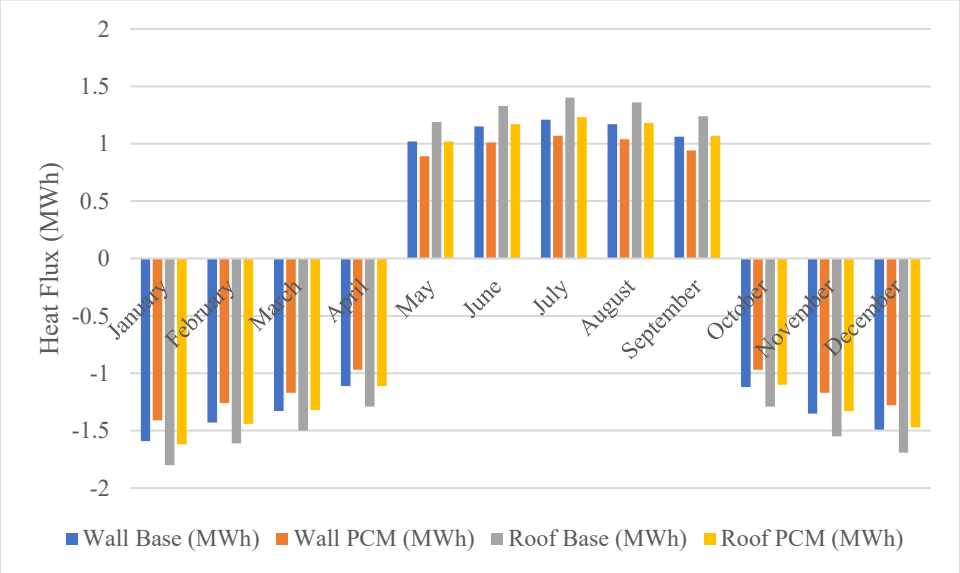

Fig. 5. Monthly heat flux values for walls and roof (Base vs. PCM)

To further elucidate seasonal effects, **Fig. 6** summarizes the cumulative heat fluxes for winter (October–April) and summer (May–September) periods. Seasonal analysis reveals that during the winter months, PCM integration reduced the cumulative wall heat loss by 1.15 MWh, from -8.41 MWh to -7.26 MWh, corresponding to a 13.7% decrease. The roof experienced a more pronounced reduction of 1.86 MWh, from -9.73 MWh to -7.87 MWh, amounting to a 19.1% decrease. In the summer season, PCM reduced the wall heat gain by 652 kWh, from +5.6 MWh to +4.95 MWh, an 11.6% reduction, while the roof heat gain decreased by 857 kWh, from +6.53 MWh to +5.67 MWh, representing a 13.1% reduction. These results highlight PCM's effective mitigation of both heat loss and gain, contributing to improved thermal regulation across seasons.

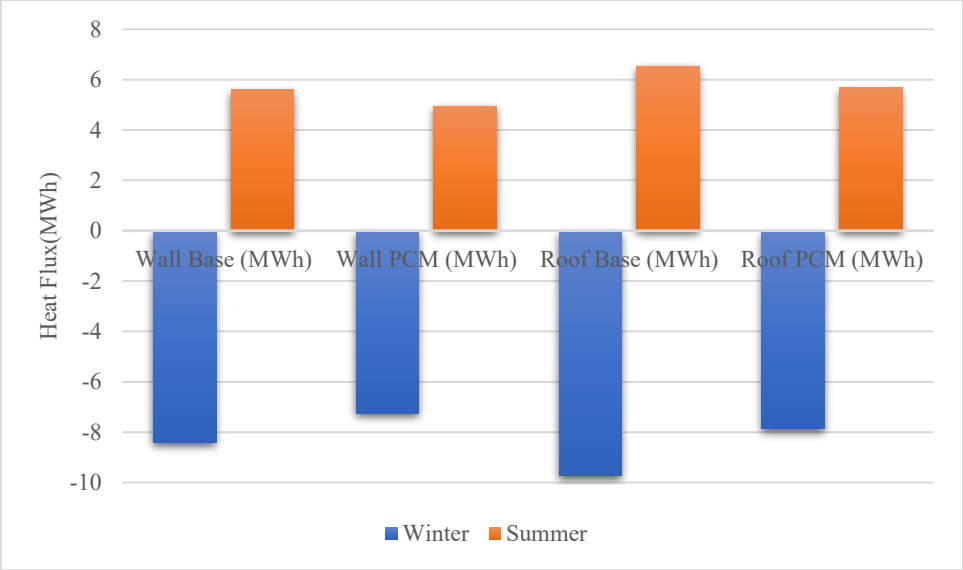

Fig. 6. Seasonal cumulative heat fluxes and percentage reductions due to PCM integration.

Annual cumulative heat fluxes, shown in Table 4, quantify the total thermal energy transferred through the building envelope components over the entire year.

On an annual basis, the total heat flux through the walls decreased from 15,915 kWh in the Base case to 13.17 MWh with PCM, a reduction of 2.745 MWh or 17.2%. The roof exhibited an even greater annual reduction of 3.955 MWh, from 18.065 MWh to 14.11 MWh, corresponding to a 21.9% decrease. Cumulatively, the building envelope's heat flux was reduced by 6.70 MWh annually, from 33.98 MWh to 27.28 MWh, representing an overall 19.7% reduction in thermal energy transfer due to PCM incorporation.

Table 4. Annual cumulative heat flux through walls and roof for Base and PCM cases.

Component	Base (MWh)	PCM (MWh)	Reduction (MWh)	Reduction (%)
Walls	15.92	13.17	2.75	17.2
Roof	18.07	14.11	3.96	21.9
Total	33.98	27.28	6.7	19.7

These results demonstrate that integrating PCM into the external walls and roofs reduces heat transfer through the building envelope, particularly during the warmest months when cooling loads peak. The roof experiences higher heat flux than the walls due to greater solar exposure, resulting in a more pronounced PCM-induced reduction in heat transfer. The effectiveness of PCM increases from the colder winter months toward the warmer months, as its melting temperature is better suited for higher temperatures.

3.2. Monthly loads of the building (Load consumption and electricity)

This section presents the monthly energy consumption of the base building in Jinan, normalized per square meter of floor area (kWh/m²). It should be noted that the values for heating, cooling, and domestic hot water (DHW) in **Fig. 1** represent thermal loads (energy demand) required to maintain indoor comfort, not the final delivered or consumed energy. No energy conversion systems have been modeled at this stage; these loads will serve as inputs for subsequent system simulations. Normalization allows for a fair comparison of energy performance across different months and facilitates benchmarking with other studies or building types. Four main categories are reported: room electricity, space heating, space cooling, and DHW. The results reflect the building's energy demand patterns in response to the local climate conditions. To quantitatively assess the effectiveness of PCM integration in reducing energy consumption and thermal loads, the energy saving efficiency is calculated using the **Eq. (6)** [46]:

$$EnergySavingEfficiency = \frac{E_{BaseCase} - E_{PCM}}{E_{BaseCase}} \quad (6)$$

Where the $E_{Base\ Case}$ is the thermal loads calculated for the nase case and the E_{PCM} is for the load demands in the PCM case.

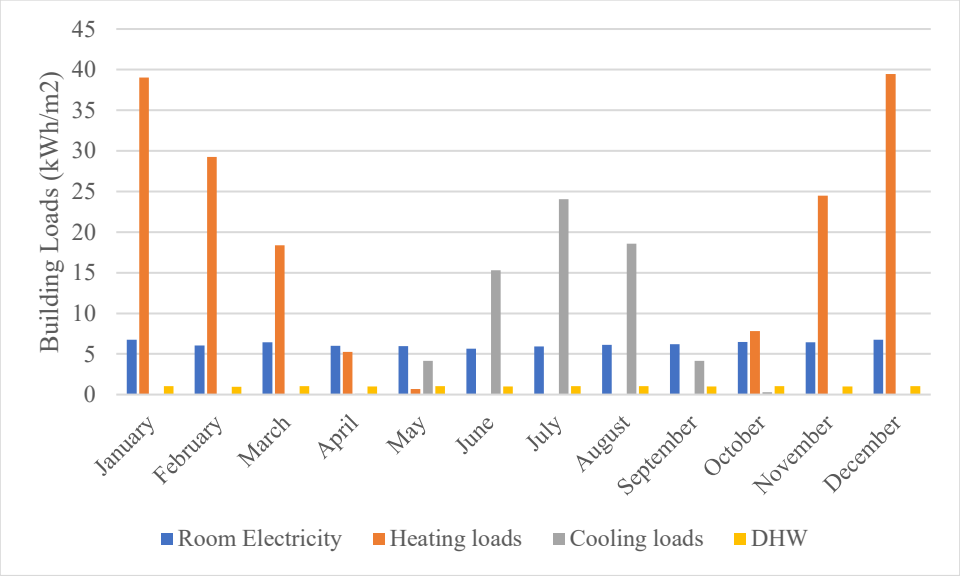

Fig. 7. summarizes the monthly normalized energy consumption of the building.

As shown in **Fig. 7**, the highest heating demand occurs in January (39.01 kWh/m²) and December (39.47 kWh/m²), reflecting the cold winter climate of Jinan. It is noteworthy that the winters in Jinan are considerably more severe than the summers, resulting in a significantly higher heating load compared to the cooling load. Consequently, the heating system must operate more intensively to maintain indoor comfort during the winter months. Heating requirements decrease significantly in the spring and autumn, reaching near zero during the summer months (June to August). Cooling demand is negligible for most of the year except during the summer, with a peak in July (24.04 kWh/m²) and a secondary maximum in August (18.59 kWh/m²), which is consistent with the hot and humid summer climate. The transition months (May and September) show moderate cooling loads, while the rest of the year has minimal or zero cooling demand. Room electricity consumption remains relatively stable throughout the year, ranging from 5.66 kWh/m² in June to 6.74 kWh/m² in January and December. This indicates that lighting and plug loads are not significantly affected by seasonal changes. DHW consumption also shows minimal seasonal variation, remaining between 0.94 and 1.04 kWh/m², suggesting consistent occupant behavior. Overall, the seasonal trends in heating and cooling loads closely match the climatic characteristics of Jinan, confirming the validity of the simulation results and the suitability of the base building model for further comparative analysis.

Fig. 8 presents the monthly normalized energy consumption of the building with PCM integration in Jinan, expressed per square meter of floor area (kWh/m²). As with the base case, the values for heating, cooling, and DHW represent thermal loads (energy demand) required to maintain indoor comfort, not the final delivered or consumed energy. No energy conversion systems have been modeled at this stage; these loads will serve as inputs for subsequent system simulations. The normalization enables a direct comparison with the base case and highlights the impact of PCM application on energy demand patterns.

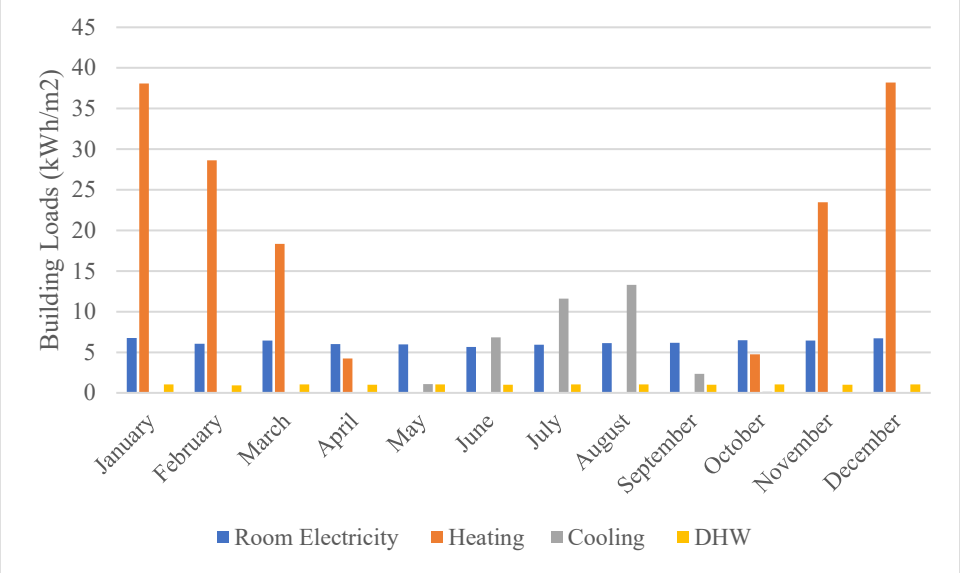

Fig. 8. summarizes the monthly normalized energy consumption of the building with PCM.

As shown in **Fig. 8**, the integration of PCM leads to a reduction in heating and cooling loads across most months compared to the base case. The highest heating demand remains in January (38.09 kWh/m²) and December (38.22 kWh/m²), but these values are slightly lower than those observed in the base scenario, indicating the effectiveness of PCM in reducing heat loss during the coldest months.

Cooling demand is also reduced, particularly in the summer months, with July (11.60 kWh/m²) and August (13.31 kWh/m²) showing substantial decreases compared to the base case. In transitional months, such as May and September, the PCM case presents significantly lower cooling loads. Room electricity and DHW loads remain essentially unchanged, as expected, since PCM primarily affects thermal loads.

Overall, the results demonstrate that PCM integration can effectively moderate both heating and cooling energy demands in Jinan's climate, especially during periods of peak thermal load, thereby enhancing the building's energy performance.

3.3. Comparative Analysis of Heating and Cooling Loads Between Base and PCM Cases

This section presents a comprehensive comparison of the monthly heating and cooling thermal loads between the Base and PCM cases for the building located in Jinan. The analysis focuses on the peak months with the highest thermal loads and the annual cumulative loads, providing a realistic and meaningful evaluation of PCM's impact on building energy demand.

3.3.1. Peak Heating Load Analysis

The peak heating loads occur in the coldest months of the year, January and December. In the Base case, the heating loads for these months are 39.01 kWh/m² and 39.47 kWh/m², respectively. With PCM integration, these values decrease to 38.09 kWh/m² in January and 38.22 kWh/m² in December, corresponding to reductions of approximately 2.4% and 3.2%. Although the percentage reductions appear modest, they represent meaningful energy savings given the high heating demand during winter in Jinan's cold climate. This reduction is attributed to PCM's ability to store thermal energy during warmer periods and release it during colder hours, thus reducing the heating load required to maintain indoor comfort.

3.3.2. Peak Cooling Load Analysis

The highest cooling loads are observed in the summer months of July and August. The Base case cooling loads are 24.04 kWh/m² and 18.59 kWh/m², respectively, while the PCM case shows significantly reduced loads of 11.60 kWh/m² in July and 13.31 kWh/m² in August. These reductions correspond to 51.7% and 28.4%, respectively. The substantial decrease in cooling demand demonstrates PCM's effectiveness in absorbing and delaying heat gains during hot periods, thereby reducing the peak cooling load and the operational burden on cooling systems.

3.3.3. Annual Heating and Cooling Load Comparison

To capture the overall impact of PCM, the annual cumulative heating and cooling loads were calculated by summing monthly values across the year:

Table 5. Annual Energy and Thermal Loads for Base and PCM Cases.

Load Type	Base Case (kWh/m²)	PCM Case (kWh/m²)	Reduction (%)
Annual Heating	180.45	157.54	12.7
Annual Cooling	70.65	38.39	45.6

The annual heating load decreases by approximately 12.7%, reflecting PCM's capacity to moderate indoor temperature fluctuations and reduce heating demand over the entire cold season. More notably, the annual cooling load is reduced by 45.6%, indicating a significant alleviation of cooling requirements due to PCM's thermal energy storage during hot months.

The discrepancy between reductions in heat flux and heating/cooling loads after PCM integration is explained by the broader nature of thermal loads, which include envelope heat transfer as well as underground heat exchange, infiltration, and solar radiation. PCM's latent heat storage delays and attenuates heat transfer, shifting loads to off-peak periods. Its thermal inertia also stabilizes indoor temperatures, indirectly reducing internal and solar gains. Thus, heating and cooling load reductions exceed those of heat flux, highlighting the need to consider dynamic thermal behavior and system-level effects when assessing PCM performance.

3.4. Indoor Air Temperature

This section presents an analysis of the indoor air temperature behavior on December 31st, considered the coldest day of the year, and July 31st, the hottest of the year, in the simulated climate. This analysis aims to evaluate the impact of PCM integration on thermal stability and occupant comfort during peak heating demands. Results illustrate the variations in outdoor temperature, indoor temperature for the baseline case (without PCM), and indoor temperature with PCM integration over 24 hours.

3.4.1. Indoor Air Temperature Performance on the Hottest Day

On July 31st, which was the hottest day of the year for Jinan, the outdoor dry-bulb temperature reached a peak of 36.44°C at 6 PM, with hourly values remaining above 35°C for more than three consecutive hours. The day exhibited typical extreme summer conditions for Jinan's temperate monsoon climate. In the base case, indoor air temperature remained relatively flat until noon (~28.25°C), after which it increased sharply, peaking at 35.15°C around 7 PM. This sharp gain of nearly 7°C during the day reflects the low thermal resistance of the untreated envelope under intense solar radiation and outdoor temperature rise. In contrast, the PCM-enhanced scenario showed a significantly dampened and delayed response: the peak indoor temperature reached only 32.77°C, indicating a reduction of ~2.4°C compared to the base case. Thermal damping was evident: the PCM absorbed latent heat during peak hours, limiting internal gains. Thermal lag was also observed: the temperature peak in the PCM case occurred 1–1.5 hours later, confirming delayed heat transfer to the interior. The difference between early afternoon (12–3 PM) and evening temperatures in the PCM model remained within 2.5°C, compared to 5.2°C in the base case, confirming PCM's role in moderating temperature swings. **Fig. 9** visually represents the hourly variations of outdoor temperature, indoor temperature for the baseline case, and indoor temperature for the PCM-integrated case on July 31st.

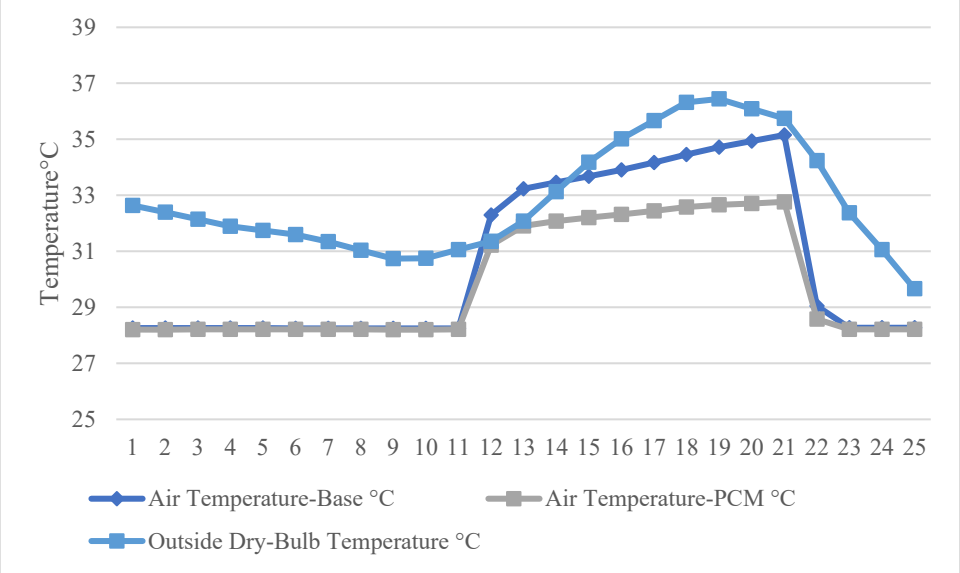

Fig. 9. Hourly temperature profiles for outdoor, indoor baseline, and PCM-integrated indoor environments on July 31st.

3.4.2. Indoor Air Temperature Performance on the Coldest Day

To evaluate PCM behavior under extreme cold conditions, the indoor air temperature profiles on December 31st—the coldest day recorded—were analyzed. On this day, the outdoor temperature reached a minimum of –12.76°C, remaining below –10°C for several continuous hours and presenting a highly challenging thermal environment for the building envelope. In the non-PCM case, indoor temperatures showed clear sensitivity to external fluctuations. The air temperature dropped from approximately 13.77°C at midnight to a low of 10.47°C by late morning. The overall thermal swing over the course of the day exceeded 3.3°C, indicating substantial overnight heat loss and inadequate buffering against extreme cold. In contrast, the PCM-integrated case exhibited a more moderated and stable temperature profile: the minimum indoor temperature was ~12.09°C, nearly 1.6°C higher than the base case. The decline in temperature was more gradual, and the early morning minimum occurred later in the day, confirming the thermal lag effect of PCM. The total thermal swing was reduced to approximately 2.2°C, suggesting an improved ability to retain heat and resist ambient temperature fluctuations. This consistent elevation and stabilization of indoor air temperature in the PCM case highlights the material's effectiveness in dampening thermal loss during winter nights and delaying cold penetration. These characteristics are especially valuable in climates like Jinan, where buildings experience intense diurnal and seasonal thermal gradients.

Fig. 10 visually represents the hourly variations of outdoor temperature, indoor temperature for the baseline case, and indoor temperature for the PCM-integrated case on December 31st.

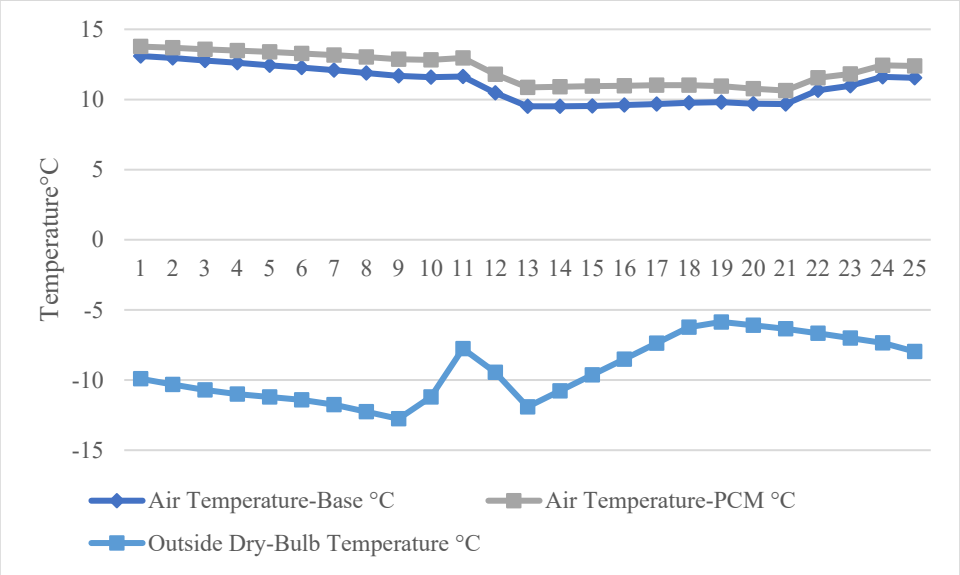

Fig. 10. Hourly temperature profiles for outdoor, indoor baseline, and PCM-integrated indoor environments on December 31st.

4. Conclusion

This study evaluates the thermal performance of a single-family residential building in Jinan, China, incorporating the phase change material InfiniteR29 within the exterior walls and roof. Using detailed hourly simulations over a full year conducted in DesignBuilder and EnergyPlus, the results indicate that PCM integration reduces the overall heat flux through the building envelope by approximately 19.7%, leading to significant savings in energy consumption. Specifically, the annual heating loads decreased by 12.7%, and cooling loads decreased by 45.6%. The PCM's effectiveness in stabilizing indoor temperatures is evidenced by a maximum indoor temperature reduction of 2.4°C during peak summer days and a delay in peak indoor temperatures, thereby enhancing thermal comfort. These findings suggest that PCM can be a practical passive strategy for energy-efficient residential design in temperate climates, though further studies are recommended to evaluate long-term performance and economic feasibility.

Incorporating PCM into the building's external walls and roof led to a substantial reduction in heat flux throughout the year. PCM reduced winter heat loss by 13.7% in walls and 19.1% in roofs, and summer heat gain by 11.6% and 13.1%, respectively. The most significant reduction was observed on the roof due to direct solar exposure. On an annual basis, the total heat flux of the building envelope decreased by 6.70 MWh—from 33.98 MWh in the Base case to 27.28 MWh, with PCM representing a 19.7% reduction as mentioned earlier.

These results confirm PCM's dual effectiveness in both heating and cooling load mitigation, supporting its value as a passive energy-saving solution for buildings located in climates similar to the studied case. Peak heating load reductions reached up to 3.2% during winter months, while peak cooling load reductions were as high as 51.7% in summer. Room electricity consumption showed no significant change, confirming that PCM primarily affects thermal loads. Although no direct thermal comfort or economic evaluation was included in this study, the demonstrated load reduction and temperature stabilization suggest strong potential for PCM integration in climate-responsive residential buildings. Future research may explore

optimized PCM selection for specific seasonal performance, as well as coupling with HVAC system sizing and energy cost analysis. Furthermore, given that Jinan experiences both hot summers and cold winters, future studies could investigate the use of dual-layer PCM systems, where materials with different melting points are applied in combination. For instance, a composite approach using low-melting-point PCM for winter activation and higher-melting-point PCM for summer activation—each at half the original thickness—may enhance year-round performance. Additionally, the placement sequence and layer positioning of PCMs within the wall or roof assembly could be optimized as a variable parameter to identify the most effective configuration for thermal buffering in transitional climates.

References

[1] Rapone, L., Li Castri, G., Lavilletta, M., Favoino, F., Perino, M., Serra, V., Double-Skin Façade with Air-PCM Latent Heat Exchanger: First Results from Experimental Campaign. In: Berardi, U. (eds) Multiphysics and Multiscale Building Physics. IABP 2024. Lecture Notes in Civil Engineering 552 (2025) Springer, Singapore. https://doi.org/10.1007/978-981-97-8305-2_61.

[2] Gonçalves, M., Figueiredo, A., Almeida, R.M.S.F., Vicente, R., Samagaio, A. (2025). Dynamic Shading Device with Phase Change Materials: A Proof-of-Concept Towards Improving Thermal Comfort. In: Berardi, U. (eds) Multiphysics and Multiscale Building Physics. IABP 2024. Lecture Notes in Civil Engineering, vol 554. Springer, Singapore. https://doi.org/10.1007/978-981-97-8313-7_37

[3] H. K. Berent, E. Cihan, and H. Demir, "Examination of effect of inclination angle on RT35 HC thermal energy storage performance with honeycomb fins of different cell sizes," Journal of Energy Storage, vol. 114, p. 115708, 2025, doi: https://doi.org/10.1016/j.est.2025.115708.

[4] A. Alasiri and M. Nasser, "Comparative analysis of PCM configurations for energy-efficient air conditioning systems: A case study in Riyadh, Saudi Arabia," Case Studies in Thermal Engineering, vol. 65, p. 105691, 2025, doi: https://doi.org/10.1016/j.csite.2024.105691.

[5] M. Alvarez-Rodriguez, M. Alonso-Martinez, I. Suarez-Ramon, and P. José García-Nieto, "Numerical model for determining the effective heat capacity of macroencapsulated PCM for building applications," Applied Thermal Engineering, vol. 242, p. 122478, 2024, doi: https://doi.org/10.1016/j.applthermaleng.2024.122478.

[6] Al-Shannaq, Refat, Monzer Daoud, Mohammed Farid, Md Wasi Ahmad, Shaheen A. Al-Muhtaseb, Mazhar Ul-Islam, Abdullah Al Saidi, and Imran Zahid, "Roles of Polymerization Temperature and Initiator Type on Thermal Properties of Rubitherm® 21 PCM Microcapsules," Micro, vol. 5, no. 2. 2025. doi: 10.3390/micro5020019.

[7] Shah, Ali Hasan, Ahmed Hassan, Shaimaa Abdelbaqi, Hamza Alnoman, Abbas Fardoun, Mahmoud Haggag, Mutassim Noor, and Mohammad Shakeel Laghari, "Parametric Optimization of Concentrated Photovoltaic-Phase Change Material as a Thermal Energy Source for Buildings," Buildings, vol. 15, no. 3. 2025. doi: 10.3390/buildings15030327.

[8] S. Sacchet, F. Valentini, M. Guidolin, R. Po, and L. Fambri, "Shape-Stabilized Phase Change Materials with Expanded Graphite for Thermal Management of Photovoltaic Cells: Selection of Materials and Preparation of Panels," Applied Sciences, vol. 15, no. 8. 2025. doi: 10.3390/app15084352.

[9] Z. Jia, S. Cunha, J. Aguiar, and C. Shi, "Enhancing the durability of concrete with construction and demolition waste aggregate through its functionalization with phase change materials (paraffin)," Cement and Concrete Composites, vol. 162, p. 106135, 2025, doi: https://doi.org/10.1016/j.cemconcomp.2025.106135.

[10] R. Gad, H. Mahmoud, S. Ookawara, and H. Hassan, "Energy, exergy, and economic assessment of thermal regulation of PV panel using hybrid heat pipe-phase change material cooling system," Journal of Cleaner Production, vol. 364, p. 132489, 2022, doi: https://doi.org/10.1016/j.jclepro.2022.132489.

[11] R. Lazzarin, M. Noro, G. Righetti, and S. Mancin, "Application of Hybrid PCM Thermal Energy Storages with and without Al Foams in Solar Heating/Cooling and Ground Source Absorption Heat Pump Plant: An Energy and Economic Analysis," Applied Sciences, vol. 9, no. 5. 2019. doi: 10.3390/app9051007.

[12] A. Kandil, M. Emam, H. Sekiguchi, and S. Nada, "Energy management of residential buildings using innovative passive techniques," Journal of Physics: Conference Series, vol. 2857, no. 1, p. 12017, 2024, doi: 10.1088/1742-6596/2857/1/012017.

[13] Gonçalves, Margarida, António Figueiredo, German Vela, Filipe Rebelo, Ricardo M. S. F. Almeida, Mónica S. A. Oliveira, and Romeu Vicente, "Effect of Macrocapsule Geometry on PCM Performance for Thermal Regulation in Buildings," Energies, vol. 18, no. 2. 2025. doi: 10.3390/en18020303.

[14] E. Mandev, "Enhancing thermoregulation in double glazed windows with PCMs and black films: An experimental study," Energy and Buildings, vol. 328, p. 115171, 2025, doi: https://doi.org/10.1016/j.enbuild.2024.115171.

[15] K. Kant, A. Shukla, and A. Sharma, "Numerical simulation of building wall incorporating phase change material for cooling load reduction," Energy and Climate Change, vol. 1, p. 100008, 2020, doi: https://doi.org/10.1016/j.egycc.2020.100008.

[16] M. Özdemir and A. Gülten, "Effect of phase change materials on building heating and cooling load considering different wall combinations," Journal of Design for Resilience in Architecture and Planning, vol. 5, no. 3 SE-Research Articles, pp. 363–377, Dec. 2024, doi: 10.47818/DRArch.2024.v5i3137.

[17] J. Krasoń, P. Miąsik, A. Starakiewicz, and L. Lichołai, "Thermal Energy Storage Possibilities in the Composite Trombe Wall Modified with a Phase Change Material," Energies, vol. 18, no. 6. 2025. doi: 10.3390/en18061433.

[18] M. Ryms and E. Klugmann-Radziemska, "Possibilities and benefits of a new method of modifying conventional building materials with phase-change materials (PCMs)," Construction and Building Materials, vol. 211, pp. 1013–1024, 2019, doi: https://doi.org/10.1016/j.conbuildmat.2019.03.277.

[19] Z. Chen, Y. Cui, H. Zheng, and Q. Ning, "Optimization and prediction of energy consumption, light and thermal comfort in teaching building atriums using NSGA-II and machine learning," Journal of Building Engineering, vol. 86, p. 108687, 2024. https://doi.org/10.1016/j.jobe.2024.108687

[20] H. Zhang, Y. Cui, H. Cai, and Z. Chen, "Optimization and prediction of office building shading devices for energy, daylight, and view consideration using genetic and BO-LGBM algorithms," Energy and Buildings, vol. 324, p. 114939, 2024. https://doi.org/10.1016/j.enbuild.2024.114939

[21] D. Wang, J. Cao, B. Zhang, K. Kong, and R. Wang, "Spatial and temporal dynamics of urban heat environment at the township scale: A case study in Jinan city, China," PLoS One, vol. 19, no. 9, p. e0307711, 2024. https://doi.org/10.1371/journal.pone.0307711

[22] X. Zhou, N. Wang, J. Zou, G. Liu, X. Zhuang, and G. Liu, "Analysis and prediction of energy consumption in office buildings with variable refrigerant flow systems: A case study," Journal of Building Engineering, vol. 97, p. 110936, 2024. https://doi.org/10.1016/j.jobe.2024.110936

[23] X. Dong, H. Xiao, M. Liu, B. Lin, and W. Wang, "An innovative Trombe wall with a solar concentrating function," Energy and Buildings, vol. 325, p. 114942, 2024. https://doi.org/10.1016/j.enbuild.2024.114942

[24] I. B. Mansir, E. H. Bani Hani, N. Farouk, A. AlArjani, H. Ayed, and D. D. Nguyen, "Comparative transient simulation of a renewable energy system with hydrogen and battery energy storage for residential applications," International journal of hydrogen energy, vol. 47, no. 62, pp. 26198–26208, 2022, doi: https://doi.org/10.1016/j.ijhydene.2022.02.092.

[25] I. B. Mansir, E. H. B. Hani, H. Ayed, and C. Diyoke, "Dynamic simulation of hydrogen-based zero energy buildings with hydrogen energy storage for various climate conditions," International journal of hydrogen energy, vol. 47, no. 62, pp. 26501–26514, 2022, doi: 10.1016/j.ijhydene.2021.12.213.

[26] Jung, S.; Han, S.; Jeoung, J.; Kim, S.; Hong, T.; Choi, J.-K.; Lee, M, "Optimal planning of building integrated photovoltaic windows through room-level economic analysis," Energy and Buildings, vol. 337, p. 115690, 2025, doi: https://doi.org/10.1016/j.enbuild.2025.115690.

[27] N. Amani, "Energy efficiency of residential buildings using thermal insulation of external walls and roof based on simulation analysis," Energy Storage and Saving, vol. 4, no. 1, pp. 48–55, 2025, doi: https://doi.org/10.1016/j.enss.2024.11.006.

[28] A. Abdeen, E. Mushtaha, A. Hussien, C. Ghenai, A. Maksoud, and V. Belpoliti, "Simulation-based multi-objective genetic optimization for promoting energy efficiency and thermal comfort in existing buildings of hot climate," Results in Engineering, vol. 21, p. 101815, 2024, doi: https://doi.org/10.1016/j.rineng.2024.101815.

[29] I. Adilkhanova, S. A. Memon, J. Kim, and A. Sheriyev, "A novel approach to investigate the thermal comfort of the lightweight relocatable building integrated with PCM in different climates of Kazakhstan during summertime," Energy, vol. 217, p. 119390, 2021, doi: https://doi.org/10.1016/j.energy.2020.119390.

[30] A. Mabrouki, Y. Bennani Karim, H. Ouadghiri Hassani, Y. Jamali, and A. Khaldoun, "A study of a passive heating design employing a Trombe wall with PCM: A numerical investigation of the semi-oceanic climate in Morocco," Materials Today: Proceedings, vol. 72, pp. 3626–3631, 2023, doi: https://doi.org/10.1016/j.matpr.2022.08.410.

[31] M. Bozorgi, S. H. Tasnim, and S. Mahmud, "Machine learning-driven hybrid cooling system for enhanced energy efficiency in multi-unit residential buildings," Energy and Buildings, vol. 336, p. 115613, 2025, doi: https://doi.org/10.1016/j.enbuild.2025.115613.

[32] C. Keles, "Evaluating the Effect of Building Envelope on Thermal Performance in Cold and Warm Climate Regions of Turkey," European Journal of Engineering Science and Technology, vol. 3, no. 1, pp. 93–104, 2020, doi: 10.33422/ejest.v3i1.165.

[33] J. E. Torres-Quezada and A. Torres-Avilés, "The Constructive Evolution of the Envelope. The Impact on Indoor Thermal Conditions in Andean Regions BT - Energetic Characterization of Building Evolution: A Multi-perspective Evaluation in the Andean Region of Ecuador," In: Torres-Quezada,

J.E. (eds) Energetic Characterization of Building Evolution. Green Energy and Technology, Cham: Springer International Publishing, 2023, pp. 49–77. doi: 10.1007/978-3-031-21598-8_2.

[34] R. Caponetto, C. Di Mari, G. Giuffrida, and F. Nocera, "Analysis of the environmental, economic, thermal and energy performances of green building technologies," Renewable Energy and Power Quality Journal, vol. 20, no. September, pp. 84–89, 2022, doi: 10.24084/repqj20.226.

[35] G. Miracco, F. Nicoletti, V. Ferraro, M. Muzzupappa, V. M. Mattanò, and F. Alberti, "Achieving nZEB goal through prefabricated buildings: Case study in Italy," Energy and Buildings, vol. 329, p. 115301, 2025, doi: https://doi.org/10.1016/j.enbuild.2025.115301.

[36] N. Soussi, M. Ammar, A. Mokni, and H. Mhiri, "Efficiency of a recycled composite material for building insulation," Construction and Building Materials, vol. 467, p. 140358, 2025, doi: https://doi.org/10.1016/j.conbuildmat.2025.140358.

[37] Mehdizadeh Marzebali, M. R., & Mohamadian, M. Techno-environmental and economic assessment of off-grid hybrid energy systems for combined cooling, heating, power, and battery-hydrogen storage. Advances in Energy Sciences and Technologies, 2025, 1(1), 28-51.

[38] A. Aldawoud, L. A. Husein, and E. S. Mushtaha, "Electrochromic glazing with nanocoating integration impact on building energy efficiency: Bibliometric analysis (1983–2023)," Energy and Buildings, vol. 330, p. 115300, 2025, doi: https://doi.org/10.1016/j.enbuild.2025.115300.

[39] A. Albatayneh, R. Albadaineh, A. Juaidi, and R. Abdallah, "Trade-off lighting to minimize the cooling loads in semi-arid climate zone," Energy and Buildings, vol. 328, p. 115100, 2025, doi: https://doi.org/10.1016/j.enbuild.2024.115100.

[40] R. Aridi and A. Yehya, "Review on the sustainability of phase-change materials used in buildings," Energy Conversion and Management: X, vol. 15, p. 100237, 2022. https://doi.org/10.1016/j.ecmx.2022.100237

[41] Mennatallah Hassan, Khaled Dewidar, Mostafa Ismail, Ashraf Nessim, Aly Abdelalim, "Optimizing Phase Change Material on Opaque Building Envelope to Reach nZEB," Civil Engineering and Architecture, Vol. 11, No. 6, pp. 3667 - 3680, 2023. DOI: 10.13189/cea.2023.110632.

[42] V. J. Reddy, M. F. Ghazali, and S. Kumarasamy, "Advancements in phase change materials for energy-efficient building construction: A comprehensive review," Journal of Energy Storage, vol. 81, p. 110494, 2024, doi: https://doi.org/10.1016/j.est.2024.110494.

[43] O. A. Ismail, M. A. Mandour, and A. H. Hussin, "Application of phase change materials (PCMs) in administrative building's envelope to improve its thermal comfort," Engineering Research Journal, vol. 184, no. 2, pp. 320–340, 2025. DOI: 10.21608/erj.2024.333777.1138

[44] S. Lingfan, G. Lin, and C. Hongbo, "Numerical simulation of composite PCM integration in prefabricated houses: Sustainable and improved energy design," Journal of Energy Storage, vol. 91, p. 111987, 2024. https://doi.org/10.1016/j.est.2024.111987

[45] C. G. Rangel, C. I. Rivera-Solorio, M. Gijón-Rivera, and S. Mousavi, "The effect on thermal comfort and heat transfer in naturally ventilated roofs with PCM in a semi-arid climate: An experimental research," Energy and Buildings, vol. 274, p. 112453, 2022. https://doi.org/10.1016/j.enbuild.2022.112453

[46] A. M. Bolteya, M. A. Elsayad, O. D. El Monayeri, and A. M. Belal, "Impact of Phase Change Materials on Cooling Demand of an Educational Facility in Cairo, Egypt," Sustainability, vol. 14, no. 23. 2022. doi: 10.3390/su142315956.